Chapter 15

Indium Nitride (InN)

15.1 STRUCTURAL PROPERTIES

15.1.1 Ionicity

Table 15.1.1 *Phillips's ionicity f_i for InN [1.1].*

f_i
0.578

[1.1] J. C. Phillips, *Bonds and Bands in Semiconductors* (Academic, New York, 1973).

15.1.2 Elemental Isotopic Abundance and Molecular Weight

- **Isotopic abundance**

Table 15.1.2 *Isotopic abundance in percent for indium and nitrogen [1.2].*

Isotope	% nat. abundance	Isotope	% nat. abundance
^{113}In	4.3	^{14}N	99.634
^{115}In	95.7	^{15}N	0.366

[1.2] D. R. Lide, *CRC Handbook of Chemistry and Physics*, 78th Edition (CRC Press, Boca Raton, 1997).

• **Molecular weight**

Table 15.1.3 *Molecular (average atomic) weight M for InN.*

M (amu)
128.825

15.1.3 Crystal Structure and Space Group

Table 15.1.4 *Crystal structure and its space and pint groups for InN.*

Crystal structure	Space group	Point group
Wurtzite (Hexagonal)	$P6_3mc$	C_{6v}^4

15.1.4 Lattice Constant and Its Related Parameters

• **Lattice constant**

Table 15.1.5 *Lattice constant (a, c) for InN at 300 K.*

a (Å)	c (Å)	Ref.
3.548	5.760	[1.3]
3.544	5.718	[1.4]
3.5480	5.760	[1.5]
3.5365	5.7039	[1.6]

[1.3] R. B. Zetterstrom, *J. Mater. Sci.* **5**, 1102 (1970).
[1.4] K. Osamura, S. Naka, and Y. Murakami, *J. Appl. Phys.* **46**, 3432 (1975).
[1.5] T. L. Tansley and C. P. Foley, *J. Appl. Phys.* **59**, 3241 (1986).
[1.6] Note that this paper reports an evidence of the narrow band-gap energy of E_0~0.9 eV [V. Yu. Davydov, A. A. Klochikhin, R. P. Seisyan, V. V. Emtsev, S. V. Ivanov, F. Bechstedt, J. Furthmüller, H. Harima, A. V. Mudryi, J. Aderhold, O. Semchinova, and J. Graul, *Phys. Status Solidi B* **229**, R1 (2002)].

• **Lattice constant and molecular density**

Table 15.1.6 *Lattice constant (a, c) and molecular density (d_M) for InN at 300 K.*

Parameter	Value
Lattice constant a (Å)	3.548
c (Å)	5.760
Molecular density d_M (10^{22} cm^{-3})	3.185

• **Crystal density**

Table 15.1.7 *Crystal density g for InN at 300 K.**

g (g/cm^3)
6.813

*Calculated using a=3.548 Å and c=5.760 Å.

15.1.5 Structural Phase Transition

Table 15.1.8 *Structural phase transition in InN at high pressures.*

Structure	Transition pressure (GPa)
Wurtzite ($P6_3mc$)	Normal pressure
Rocksalt (NaCl)	12.1 [1.7]
	23.0 [1.8]
	14.4 [1.9]

[1.7] M. Ueno, M. Yoshida, A. Onodera, O. Shimomura, and K. Takemura, *Phys. Rev. B* **49**, 14 (1994).
[1.8] P. Perlin, I. Gorczyca, I. Gregory, T. Suski, N. E. Christensen, and A. Polian, *Jpn. J. Appl. Phys.* **32-1** (Suppl.), 334 (1993).
[1.9] S. Uehara, T. Masamoto, A. Onodera, M. Ueno, O. Shimomura, and K. Takemura, *J. Phys. Chem. Solids* **58**, 2093 (1997).

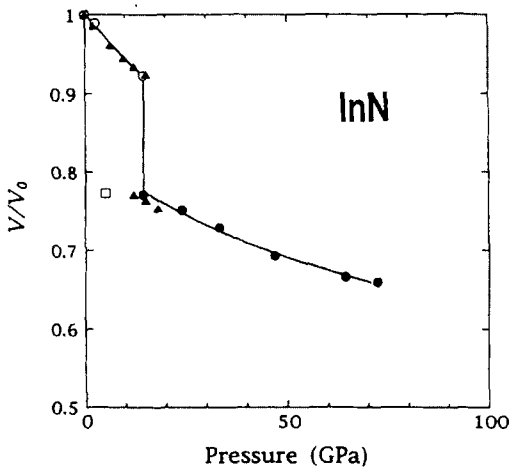

Fig. 15.1.1 Measured equation of state for InN. [From S. Uehara, T. Masamoto, A. Onodera, M. Ueno, O. Shimomura, and K. Takemura, *J. Phys. Chem. Solids* **58**, 2093 (1997).]

15.1.6 Cleavage Plane

Table 15.1.9 *Crystallographic plane most readily cleaved for InN.**

Cleavage plane
$(11\bar{2}0)$, $(10\bar{1}0)$

*Expected.

15.2 THERMAL PROPERTIES

15.2.1 Melting Point and Its Related Parameters

Table 15.2.1 *Melting point T_m and its related parameters for InN [2.1].*

Parameter	Value
Melting point T_m (K)	2146
Heat of fusion ΔH_m (kcal/mol)	14.1
Entropy of fusion ΔS_m (cal/mol K)	10.19

[2.1] Calculated [J. A. Van Vechten, *Phys. Rev. B* **7**, 1479 (1973)].

15.2.2 Specific Heat

Table 15.2.2 *Specific heat C_p (at constant pressure) for InN (in J/g K) [2.2].*

Temperature (K)	C_p (J/g K)	Temperature (K)	C_p (J/g K)
153	1.188	233	1.809
163	1.265	243	1.886
173	1.343	253	1.964
183	1.421	263	2.042
193	1.498	273	2.119
203	1.576	283	2.197
213	1.653	293	2.274
223	1.731		

[2.2] The data are taken from tabulation by S. Krukowski, M. Leszczynski, and S. Porowski [in *Properties, Processing and Applications of Gallium Nitride and Related Semiconductors*, EMIS Datareviews Series No. 23, edited by J. H. Edgar, S. Strite, I. Akasaki, H. Amano, and C. Wetzel (INSPEC, London, 1999), p. 21].

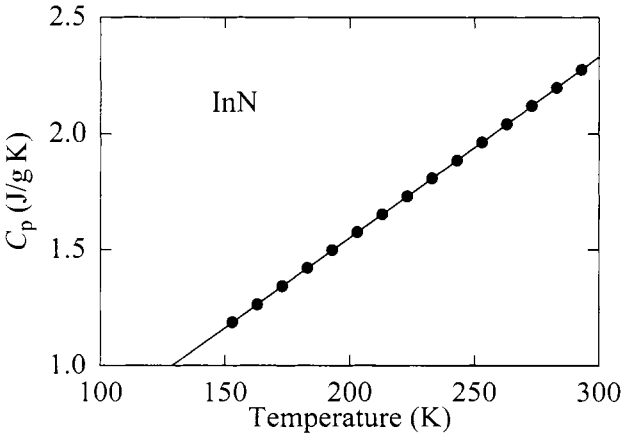

Fig. 15.2.1 Specific heat C_p (at constant pressure) versus temperature for InN. The data are taken from S. Krukowski, M. Leszczynski, and S. Porowski [in *Properties, Processing and Applications of Gallium Nitride and Related Semiconductors*, EMIS Datareviews Series No. 23, edited by J. H. Edgar, S. Strite, I. Akasaki, H. Amano, and C. Wetzel (INSPEC, London, 1999), p. 21]. The solid line represents the least-squares fit with $C_p = 7.76 \times 10^{-3} T$ (T in K; C_p in J/g K).

15.2.3 Debye Temperature

Table 15.2.3 *Debye temperature θ_D for InN [2.3].*

Temperature (K)	θ_D (K)	Temperature (K)	θ_D (K)
0	355	140	570
10	329	160	593
20	308	180	616
25	299	200	631
30	308	250	656
40	326	300	674
50	360	400	692
60	384	500	701
80	442	600	702
100	493	900	702
120	535	1200	702

[2.3] V. Yu. Davydov, V. V. Emtsev, I. N. Goncharuk, A. N. Smirnov, V. D. Petrikov, V. V. Mamutin, V. A. Vekshin, S. V. Ivanov, M. B. Smirnov, and T. Inushima, *Appl. Phys. Lett.* **75**, 3297 (1999).

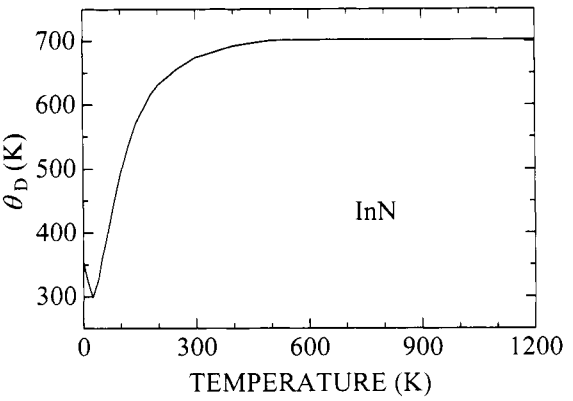

Fig. 15.2.2 Debye temperature θ_D for InN. The data are obtained from V. Yu. Davydov, V. V. Emtsev, I. N. Goncharuk, A. N. Smirnov, V. D. Petrikov, V. V. Mamutin, V. A. Vekshin, S. V. Ivanov, M. B. Smirnov, and T. Inushima [*Appl. Phys. Lett.* **75**, 3297 (1999)].

15.2.4 Thermal Expansion Coefficient

Table 15.2.4 *Thermal expansion coefficient α_{th} for InN [2.4].*

Temperature (K)	α_{th} (10^{-6} K^{-1})	
	α_a	α_c
50	0.711	0.543
100	2.288	1.683
150	3.110	2.258
200	3.501	2.526
250	3.708	2.668
298	3.826	2.748
300	3.830	2.751
350	3.909	2.804
400	3.962	2.839
450	4.002	2.864
500	4.031	2.885
550	4.055	2.900
600	4.074	2.911
650	4.090	2.921
700	4.104	2.930
750	4.117	2.938
800	4.127	2.944

[2.4] K. Wang and R. R. Reeber, *Appl. Phys. Lett.* **79**, 1602 (2001).

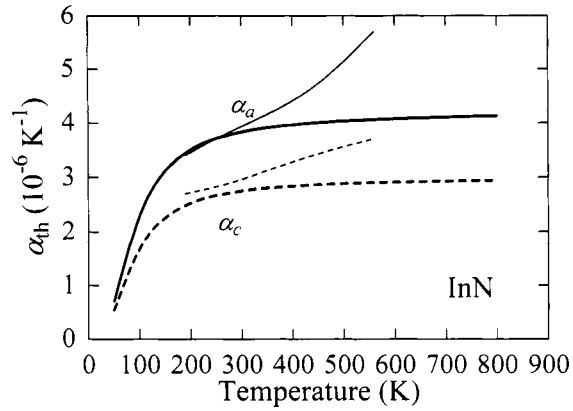

Fig. 15.2.3 Thermal expansion coefficient α_{th} versus temperature for InN. The data are taken from K. Wang and R. R. Reeber [heavy lines, *Appl. Phys. Lett.* **79**, 1602 (2001)] and from T. L. Tansley [light lines, in *Properties of Group III Nitrides*, EMIS Datareviews Series No. 11, edited by J. H. Edgar (INSPEC, London, 1994), p. 35].

15.2.5 Thermal Conductivity and Diffusivity

Table 15.2.5 *Thermal conductivity K for InN at 300 K.*

K (W/cm K)	Comment
0.8±0.2	Estimated [2.5]
0.45	InN ceramics [2.6]

[2.5] G. A. Slack, R. A. Tanzilli, R. O. Pohl, and J. W. Vandersande, *J. Phys. Chem. Solids* **48**, 641 (1987).
[2.6] S. Krukowski, A Witek, J. Adamczyk, J. Jun, M. Bockowski, I. Grzegory, B. Lucznik, G. Nowak, M. Wróblewski, A. Presz, S. Gierlotka, S. Stelmach, B. Palosz, S. Porowski, and P. Zinn, *J. Phys. Chem. Solids* **59**, 289 (1998).

15.3 ELASTIC PROPERTIES

15.3.1 Elastic Constant

• Theoretical value

Table 15.3.1 *Theoretical elastic stiffness constant C_{ij} for InN.*

C_{ij} (10^{11} dyn/cm^2)						Ref.
C_{11}	C_{12}	C_{13}	C_{33}	C_{44}	C_{66}	
27.1	12.4	9.4	20.0	4.6	7.4	[3.1]
24.3	7.19	5.25	26.3	7.23	8.6	[3.2]
22.3	11.5	9.2	22.4	4.8	5.4	[3.3]
27.1	12.4	9.4	20.0	4.6	7.4	[3.4]
29.75	10.74	10.87	25.05	8.94	9.51	[3.5]

[3.1] K. Kim, W. R. L. Lambrecht, and B. Segall, *Phys. Rev. B* **53**, 16310 (1996).
[3.2] T. Azuhata, T. Sota, and K. Suzuki, *J. Phys.: Condens. Matter* **8**, 3111 (1996).
[3.3] A. F. Wright, *J. Appl. Phys.* **82**, 2833 (1997).
[3.4] M. van Schilfgaarde, A. Sher, and A.-B. Chen, *J. Cryst. Growth* **178**, 8 (1997).
[3.5] J. A. Chisholm, D. W. Lewis, and P. D. Bristowe, *J. Phys.: Condens. Matter* **11**, L235 (1999).

• Room-temperature value

Table 15.3.2 *Elastic stiffness (C_{ij}) and compliance constants (S_{ij}) for InN at 300 K [3.6].*

C_{ij} (10^{11} dyn/cm^2)					
C_{11}	C_{12}	C_{13}	C_{33}	C_{44}	C_{66}*[1]
19.0±0.7	10.4±0.3	12.1±0.7	18.2±0.6	0.99±0.11	4.3
S_{ij} (10^{-13} cm^2/dyn)*[2]					
S_{11}	S_{12}	S_{13}	S_{33}	S_{44}	S_{66}*[1]
9.57	−2.06	−4.99	12.1	101	23.3

[3.6] X-ray diffraction [A. U. Sheleg and V. A. Savastenko, *Inorg. Mater.* **15**, 1257 (1979)].
*[1] $C_{66}=\frac{1}{2}(C_{11}-C_{12})$; $S_{66}=2(S_{11}-S_{12})$.
*[2] Calculated from C_{ij} values.

15.3.2 Third-Order Elastic Constant

No detailed data are available for InN.

15.3.3 Young's Modulus, Poisson's Ratio, and Similar

• Young's modulus

Table 15.3.3 *Young's modulus Y for InN at 300 K.* *

Direction	Y (10^{12} dyn/cm^2)
$c \perp l$	1.04
$c \parallel l$	0.83

*Calculated using S_{11}=9.57×10^{-13} and S_{33}=1.21×10^{-12} cm^2/dyn.
l: directional vector.

• Poisson's ratio

Table 15.3.4 *Poisson's ratio P for InN at 300 K.* *

Direction	P
$c \perp l$	0.38
$c \parallel l$	0.40

*Obtained from a definition B_u=Y/[3(1-2P)], where B_u and Y are bulk and Young's moduli, respectively.
l: directional vector.

• Bulk modulus, shear modulus, etc.

Table 15.3.5 *Bulk modulus, B_u, pressure derivative of B_u, dB_u/dp, and linear compressibility, C_o, for InN at 300 K.*

Parameter	Value
B_u (10^{12} dyn/cm^2)	1.39 [3.7]
dB_u/dp	12.7 [3.8]
C_o (10^{-13} cm^2/dyn)	
$c \perp l$	2.52 [3.7]
$c \parallel l$	2.12 [3.7]

[3.7] Calculated using C_{11}=1.90×10^{12} dyn/cm^2, C_{12}=1.04×10^{12} dyn/cm^2, C_{13}=1.21×10^{12} dyn/cm^2, C_{33}=1.82×10^{12} dyn/cm^2, S_{11}=9.57×10^{-13} cm^2/dyn, S_{12}= –2.06×10^{-13} cm^2/dyn, S_{13}= –4.99×10^{-13} cm^2/dyn, and S_{33}=1.21×10^{-12} cm^2/dyn.
[3.8] Exper. [see, C. Stampfl and C. G. Van de Walle, *Phys. Rev. B* **59**, 5521 (1999)].
l: directional vector.

15.3.4 Microhardness

Table 15.3.6 *Microhardness H for InN.*

H (GPa)
10±0.5 [3.9]

[3.9] (0001) basal plane [Q. Guo and A. Yoshida, *Jpn. J. Appl. Phys.* **33**, 90 (1994)].

15.3.5 Sound Velocity

Table 15.3.7 *Sound velocity propagating in InN at 300 K.* LA=longitudinal acoustic; TA1, TA2=transverse acoustic.*

Propagation direction $\boldsymbol{a}$	Direction of polarization π	Mode	Sound velocity (10^5 cm/s)
$\boldsymbol{a} \parallel c$	$\pi \parallel c$	LA	5.17
$\boldsymbol{a} \parallel c$	$\pi \perp c$	TA1, TA2	1.21
$\boldsymbol{a} \perp c$	$\pi \perp c$	LA	5.28
$\boldsymbol{a} \perp c$	$\pi \perp c$	TA1	2.51
$\boldsymbol{a} \perp c$	$\pi \parallel c$	TA2	1.21

*Calculated using $C_{11}=1.90\times10^{12}$ dyn/cm^2, $C_{12}=1.04\times10^{12}$ dyn/cm^2, $C_{33}=1.82\times10^{12}$ dyn/cm^2, $C_{44}=9.9\times10^{10}$ dyn/cm^2, and $g=6.813$ g/cm^3.

15.4 PHONONS AND LATTICE VIBRONIC PROPERTIES

15.4.1 Phonon Dispersion Relation

• Dispersion curves and phonon density of states

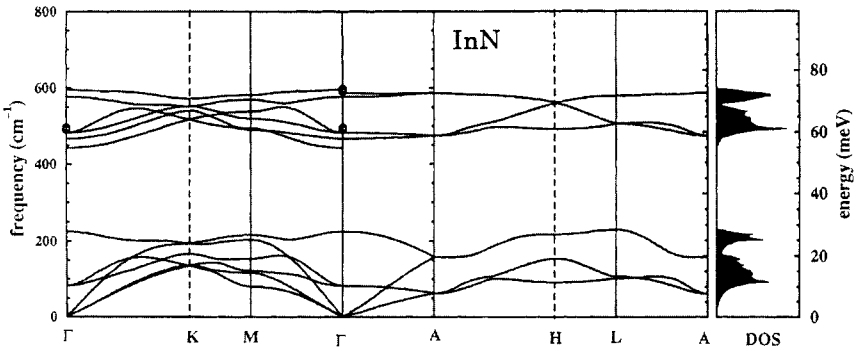

Fig. 15.4.1 Phonon dispersion curves and density of states (DOS) in InN. The symbols represent the Raman data. [From C. Bungaro, K. Rapcewicz, and J. Bernholc, *Phys. Rev. B* **61**, 6720 (2000).]

15.4.2 Phonon Frequency

Table 15.4.1 *Long-wavelength ($q \to 0$) phonon frequencies for InN at 300 K.*

Phonon frequency (cm^{-1})						Ref.
E_2 low	A_1 (TO)	E_2 high	E_1 (TO)	A_1 (LO)	E_1 (LO)	
		495		596		[4.1]
87	447	488	476	586	593	[4.2]
	472			586		[4.3]
87	480	488	476	580	570	[4.4]
	445±2	488±1	472±2	588±1		[4.5]
	443	491	475	591		[4.6]
87	457	490	475	588	582	Mean value

[4.1] H.-J. Kwon, Y.-H. Lee, O. Miki, H. Yamano, and A. Yoshida, *Appl. Phys. Lett.* **69**, 937 (1996).
[4.2] V. Yu. Davydov, V. V. Emtsev, I. N. Goncharuk, A. N. Smirnov, V. D. Petrikov, V. V. Mamutin, V. A. Vekshin, and S. V. Ivanov, *Appl. Phys. Lett.* **75**, 3297 (1999).
[4.3] G. Kaczmarczyk, A. Kaschner, S. Reich, A. Hoffmann, C. Thomsen, D. J. As, A. P. Lima, D. Schikora, K. Lischka, R. Averbeck, and H. Riechert, *Appl. Phys. Lett.* **76**, 2122 (2000).
[4.4] T. Inushima, T. Shiraishi, and V. Yu. Davydov, *Solid State Commun.* **110**, 491 (1999).
[4.5] J. S. Dyck, K. Kim, S. Limpijumnong, W. R. L. Lambrecht, K. Kash, and J. C. Angus, *Solid State Commun.* **114**, 355 (2000).
[4.6] F. Agulló-Rueda, E. E. Mendez, B. Bojarczuk, and S. Guha, *Solid State Commun.* **115**, 19 (2000).

15.4.3 Mode Grüneisen Parameter

No detailed data are available for InN.

15.4.4 Phonon Deformation Potential

No detailed data are available for InN.

15.5 COLLECTIVE EFFECTS AND RELATED PROPERTIES

15.5.1 Piezoelectric Constant

Table 15.5.1 *Theoretically obtained piezoelectric constant e_{ij} for InN.*

e_{ij} (C/m^2)			Comment
e_{15}	e_{31}	e_{33}	
	−0.41	0.81	Berry-phase approach [5.1]
	−0.52	1.09	Local density approximation [5.2]
	−0.41	0.81	Generalized gradient approximation [5.2]

[5.1] F. Bernardini, V. Fiorentini, and D. Vanderbilt, *Phys. Rev. B* **63**, 193201 (2001).
[5.2] A. Zoroddu, F. Bernardini, P. Ruggerone, and V. Fiorentini, *Phys. Rev. B* **64**, 45208 (2001).

15.5.2 Fröhlich Coupling Constant

Table 15.5.2 *Fröhlich coupling constant α_F of InN [5.3].*

α_F
0.24

[5.3] See, V. W. L. Chin, T. L. Tansley, and T. Osotchan, *J. Appl. Phys.* **75**, 7365 (1994).

15.6 ENERGY-BAND STRUCTURE: ENERGY-BAND GAPS

15.6.1 Basic Properties

• Electronic energy-band structure

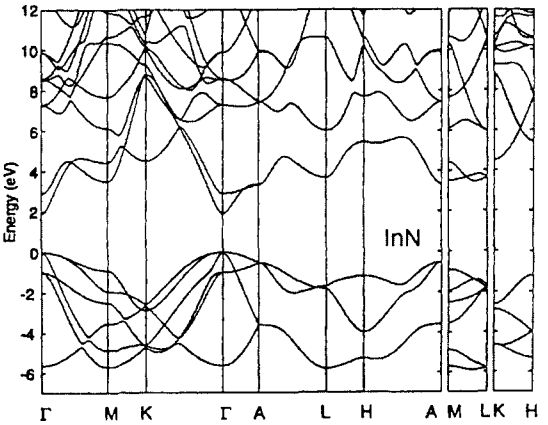

Fig. 15.6.1 Electronic energy-band structure of InN as calculated with the pseudopotential method. [From E. Bellotti, B. Doshi, K. F. Brennan, and P. P. Ruden, *Mat. Res. Soc. Symp. Proc.* **537**, G6.59 (1999).]

• Electronic density of states

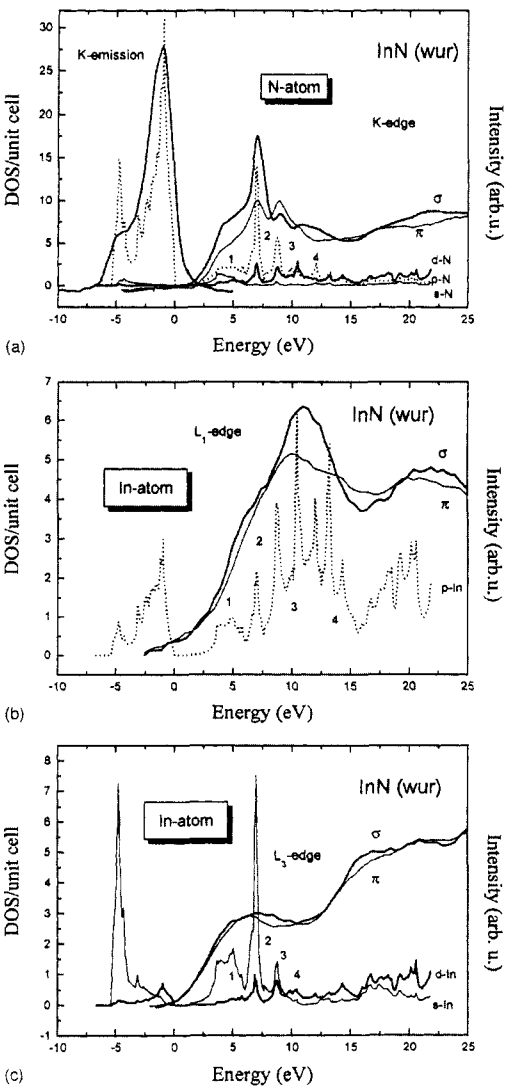

Fig. 15.6.2 Projected density of states (PDOS) for InN (*s*, thin line; *p*, dotted line; *d*, thick line). (a) Projected on the N atom and compared with N *K* emission and absorption spectra measured for π and σ polarization geometry. (b) Projected on the In atom: *p* PDOS compared with In L_1 absorption spectra measured for π and σ polarization geometry. (c) Projected on the In atom: *s* and *d* PDOS compared with In L_3 absorption spectra measured for π and σ polarization geometry. [From K. Lawniczak-Jablonska, T. Suski, I. Gorczyca, N. E. Christensen, K. E. Attenkofer, R. C. C. Perera, E. M. Gullikson, J. H. Underwood, D. L. Ederer, and Z. L. Weber, *Phys. Rev. B* **61**, 16623 (2000).]

• **Energy eigenvalue**

Table 15.6.1 *Energy eigenvalues at the critical points for the valence and first few conduction bands of InN calculated in the local-density approximation [6.1].*

Critical point	Level	Value (eV)	Critical point	Level	Value (eV)
Γ	Γ_1^v	−14.9	L	$L_{1,3}^v$	−11.2
	Γ_3^v	−11.3		$L_{1,3}^v$	−5.6
	Γ_3^v	−5.9		$L_{2,4}^v$	−1.7
	Γ_5^v	−0.9		$L_{1,3}^v$	−1.6
	Γ_5^v	−0.9		$L_{1,3}^c$	5.1
	Γ_6^v	0.0		$L_{1,3}^c$	8.4
	Γ_6^v	0.0			
	Γ_2^v	0.0			
	Γ_1^c	1.4			
	Γ_3^c	4.3			
	Γ_1^c	9.1			
	Γ_6^c	11.6			
K	K_3^v	−10.8	A	$A_{1,3}^v$	−12.7
	K_3^v	−10.8		$A_{1,3}^v$	−3.4
	K_1^v	−4.2		$A_{5,6}^v$	−0.5
	K_3^v	−4.2		$A_{5,6}^v$	−0.5
	K_3^v	−4.0		$A_{1,3}^c$	3.9
	K_2^v	−2.2		$A_{5,6}^c$	9.2
	K_3^v	−2.2			
	K_3^v	−1.8			
	K_2^c	6.7			
	K_1^c	7.3			
	K_3^c	7.4			
	K_3^c	8.1			
M	M_1^v	−11.4			
	M_3^v	−10.9			
	M_1^v	−5.5			
	M_3^v	−4.6			
	M_1^v	−3.5			
	M_2^v	−2.4			
	M_3^v	−1.8			
	M_4^v	−0.9			
	M_1^c	5.6			
	M_3^c	6.1			
	M_3^c	7.2			
	M_1^c	8.4			

[6.1] M. van Schilfgaarde, A. Shear, and A.-B. Chen, *J. Cryst. Growth* **178**, 8 (1997).

15.6.2 E_0-Gap Region

• Temperature dependence

Table 15.6.2 *$E_{0\alpha}$-gap (α=A, B, or C) energies for InN determined at various temperatures.*

Temperature (K)	$E_{0\alpha}$ (eV)	Comment
14	>1.86	n~7×10^{20} cm^{-3} [6.2]
78	2.0	[6.3]
300	1.95	[6.3]
	1.7	n~6×10^{20} cm^{-3} [6.4]
	2.05±0.1	n~$(2-3)\times10^{20}$ cm^{-3} [6.5]
	1.89	$n\leq10^{17}$ cm^{-3} [6.6]
	1.70±0.02	n~10^{20} cm^{-3} [6.7]
	1.70±0.02	n~10^{20} cm^{-3} [6.8]
	1.9	[6.9]
	1.97	[6.10]
300	1.89	Recommended ([6.11])*

[6.2] T. Inushima, T. Yaguchi, A. Nagase, A. Iso, andT . Shiraishi, *Inst. Phys. Conf. Ser.* **142**, 971 (1996).
[6.3] K. Osamura, S. Naka, and Y. Murakami, *J. Appl. Phys.* **46**, 3432 (1975).
[6.4] J. W. Trainor and K. Rose, *J. Electron. Mater.* **3**, 821 (1974).
[6.5] V. A. Tyagaĭ, A. M. Evstigneev, A. N. Krasiko, A. F. Andreeva, and V. Ya. Malakhov, *Sov. Phys. Semicond.* **11**, 1257 (1978).
[6.6] T. L. Tansley and C. P. Foley, *J. Appl. Phys.* **59**, 3241 (1986).
[6.7] B. T. Sullivan, R. R. Parsons, K. L. Westra, and M. J. Brett, *J. Appl. Phys.* **64**, 4144 (1988).
[6.8] K. L. Westra and M. J. Brett, *Thin Solid Films* **192**, 227 (1990).
[6.9] A. Wakahara, T. Tsuchiya, and A. Yoshida, *Vacuum* **41**, 1071 (1990).
[6.10] Q. Guo and A. Yoshida, *Jpn. J. Appl. Phys.* **33**, 2453 (1994).
[6.11] M. Leroux and B. Gil, in *Properties, Processing and Applications of Gallium Nitride and Related Semiconductors*, EMIS Datareviews Series No. 23, edited by J. H. Edgar, S. Strite, I. Akasaki, H. Amano, and C. Wetzel (INSPEC, London, 1999), p. 117.

*Note that very recent studies suggest an evidence of the narrow band-gap energy of E_0~1.1 eV [T. Inushima, V. V. Mamutin, V. A. Vekshin, S. V. Ivanov, T. Sakon, M. Motokawa, and S. Ohoya, *J. Cryst. Growth* **227-228**, 481 (2001)]; ~0.9 eV [V. Yu. Davydov, A. A. Klochikhin, R. P. Seisyan, V. V. Emtsev, S. V. Ivanov, F. Bechstedt, J. Furthmüller, H. Harima, A. V. Mudryi, J. Aderhold, O. Semchinova, and J. Graul, *Phys. Status Solidi B* **229**, R1 (2002)]; ~0.7 eV [V. Yu. Davydov, A. A. Klochikhin, V. V. Emtsev, S. V. Ivanov, V. V. Vekshin, F. Bechstedt, J. Furthmüller, H. Harima, A. V. Mudryi, A. Hashimoto, A. Yamamoto, J. Aderhold, J. Graul, and E. E. Haller, *Phys. Status Solidi B* **230**, R4 (2002)]; ~(0.7–0.8) eV [J. Wu, W. Walukiewicz, K. M. Yu, J. W. Ager III, E. E. Haller, H. Lu, W. J. Schaff, Y. Saito, and Y. Nanishi, *Appl. Phys. Lett.* **80**, 3967 (2002); J. Wu, W. Walukiewicz, W. Shan, K. M. Yu, J. W. Ager III, E. E.Haller, H. Lu, and W. J. Schaff, *Phys. Rev. B* **66**, 201403 (2002)]; 0.7–1.0 eV [T. Matsuoka, H. Okamoto, M. Nakao, H. Harima, and E. Kurimoto, *Appl. Phys. Lett.* **81**, 1246 (2002)].

Table 15.6.3 *Empirical equation for the $E_{0\alpha}$-gap (α=A, B, or C) energy variation with temperature T for InN.*

$$E_{0\alpha}(T) = E_{0\alpha}(0) - \frac{\alpha T^2}{T + \beta}$$

Parameter			Comment
$E_{0\alpha}(0)$ (eV)	α (10^{-4} eV/K)	β (K)	
1.915 (*A*) [6.12]	2.87	631	MOCVD-grown on Al_2O_3, T=0–300 K [6.13]
1.915 (*A*) [6.12]	2.45	624	MOCVD-grown on Al_2O_3, T=0–300 K [6.14]

[6.12] M. Leroux and B. Gil, in *Properties, Processing and Applications of Gallium Nitride and Related Semiconductors*, EMIS Datareviews Series No. 23, edited by J. H. Edgar, S. Strite, I. Akasaki, H. Amano, and C. Wetzel (INSPEC, London, 1999), p. 117.
[6.13] A. Wakahara, T. Tsuchiya, and A. Yoshida, *Vacuum* **41**, 1071 (1990).
[6.14] Q. Guo and A. Yoshida, *Jpn. J. Appl. Phys.* **33**, 2453 (1994).

Table 15.6.4 *Empirical equation for the $E_{0\alpha}$-gap (α=A, B, or C) energy variation with temperature T for InN.*

$$E_{0\alpha}(T) = E_B - \frac{a_B}{\exp(\Theta / T) - 1}$$

Parameter			Comment
E_B (eV)	a_B (meV)	Θ (K)	
1.915 (*A*) [6.15]	87.8	466	MOCVD-grown on Al_2O_3, T=0–300 K [6.16]

[6.15] M. Leroux and B. Gil, in *Properties, Processing and Applications of Gallium Nitride and Related Semiconductors*, EMIS Datareviews Series No. 23, edited by J. H. Edgar, S. Strite, I. Akasaki, H. Amano, and C. Wetzel (INSPEC, London, 1999), p. 117.
[6.16] Q. Guo and A. Yoshida, *Jpn. J. Appl. Phys.* **33**, 2453 (1994).

Table 15.6.5 *Empirical equation for the $E_{0\alpha}$-gap (α=A, B, or C) energy variation with temperature T for InN.*

$$E_{0\alpha}(T) = E_{0\alpha}(0) - \frac{\alpha \Theta_p}{2}\left[\sqrt[p]{1 + \left(\frac{2T}{\Theta_p}\right)^p} - 1\right]$$

$E_{0\alpha}(0)$ (eV)	p	α (meV/K)	Θ_p (K)	Comment
1.994	2.9	0.21	453	T=4–300 K [6.17]

[6.17] R. Pässler, *Phys. Status Solidi B* **216**, 975 (1999).

Table 15.6.6 *Empirical equation for the $E_{0\alpha}$-gap (α=A, B, or C) energy variation with temperature T for InN.*

$$E_{0\alpha}(T) = E_{0\alpha}(0) - \alpha \sum_{i=1,2} \frac{W_i \Theta_i}{\exp(\Theta_i / T) - 1}$$

$E_{0\alpha}(0)$ (eV)	α (10^{-4} eV/K)	Θ_1 (K)	Θ_2 (K)	W_1	W_2	Comment
1.994	2.2	145	626	0.14	0.86	T=4–300 K [6.18]

[6.18] R. Pässler, *J. Appl. Phys.* **89**, 6235 (2001).

- **Pressure dependence**

Table 15.6.7 *Empirical equation for the $E_{0\alpha}$-gap (α=A, B, or C) energy variation with pressure p for InN.*

$$E_{0\alpha}(p) = E_{0\alpha}(0) + ap + bp^2$$

Parameter			Comment
$E_{0\alpha}(0)$ (eV)	a (10^{-2} eV/GPa)	b (10^{-4} eV/GPa^2)	
2.04	3.3	−5.5	Calc. [6.19]

[6.19] N. E. Christensen and I. Gorczyca, *Phys. Rev. B* **50**, 4397 (1994).

- **Temperature and/or pressure coefficient**

Table 15.6.8 *Linear temperature and pressure coefficients of the excitonic energy gap $E_{0\alpha}$ (α=A, B, or C) for InN.*

Coefficient	Value	Comment
$dE_{0\alpha}/dT$ (10^{-4} eV/K)	−1.8	Estimated from [6.20]
	−1.3	T=150–300 K [6.21]
$dE_{0\alpha}/dp$ (10^{-2} eV/GPa)	2.5	Calc. [6.22]
	2.0	Exper. [6.22]
	1.9	Calc. [6.23]

[6.20] K. Osamura, S. Naka, and Y. Murakami, *J. Appl. Phys.* **46**, 3432 (1975).
[6.21] Q. Guo and A. Yoshida, *Jpn. J. Appl. Phys.* **33**, 2453 (1994).
[6.22] P. Perlin, I. Gorczyca, H. Teisseyre, T. Suski, E. Litwin-Staszewska, S. Porowski, I. Grzegory, and N. E. Christensen, *Acta Phys. Polon. A* **82**, 674 (1992).
[6.23] K. Kim, W. R. L. Lambrecht, and B. Segall, *Phys. Rev. B* **53**, 16310 (1996).

- **Doping dependence**

Table 15.6.9 *Empirical equation for the excitonic energy gap $E_{0\alpha}$ (α=A, B, or C) with doping for InN [6.24].*

$$E_{0\alpha}(n) = E_{0\alpha}(0) + an^{1/3}$$

$E_{0\alpha}(0)$ (eV)	a (eV cm)
1.89	2.1×10^{-8}

[6.24] T. L. Tansley and C. P. Foley, *J. Appl. Phys.* **59**, 3241 (1986).

• **Crystal-field and spin–orbit–splitoff energies**

Table 15.6.10 *Theoretical crystal-field and spin-orbit–splitoff energies Δ_1, Δ_2, and Δ_3 for InN (in meV). Note that in the quasi-cubic approximation, $\Delta_{cr}=\Delta_1$ and $\Delta_{so}=3\Delta_2=3\Delta_3$.*

Δ_1 (Δ_{cr})	Δ_2	Δ_3	Δ_{so}	Ref.
41			1	[6.25]
25			1	[6.26]
57			11	[6.27]
37.3	3.7			[6.28]

[6.25] S.-H. Wei and A. Zunger, *Appl. Phys. Lett.* **69**, 2719 (1996).
[6.26] W. W. Chow, A. F. Wright, A. Girndt, F. Jahnke, and S. W. Koch, *Mat. Res. Soc. Symp. Proc.* **468**, 487 (1997).
[6.27] S. K. Pugh, D. J. Dugdale, S. Brand, and R. A. Abram, *Semicond. Sci. Technol.* **14**, 23 (1999).
[6.28] D. J. Dugdale, S. Brand, and R. A. Abram, *Phys. Rev. B* **61**, 12933 (2000).

15.6.3 Higher-Lying Direct Gap

• **Room-temperature value**

Table 15.6.11 *Higher-lying direct-gap energies for InN measured at room temperature.*

Band gap	Possible transition [a]	Value (eV)	
		a	b
E_1	$\Gamma\rightarrow\Gamma$, U→U, M→M, H→H	4.7 ($\boldsymbol{E}\perp c$)	5.0 ($\boldsymbol{E}\perp c$)
		4.95 ($\boldsymbol{E}\perp c$)	
		5.4 ($\boldsymbol{E}\parallel c$)	
E_2	K→K	7.2 ($\boldsymbol{E}\perp c$)	7.6 ($\boldsymbol{E}\perp c$)
E_3	$\Gamma\rightarrow\Gamma$	8.9 ($\boldsymbol{E}\perp c$)	8.6 ($\boldsymbol{E}\perp c$)

[a] C. P. Foley and T. L. Tansley, *Phys. Rev. B* **33**, 1430 (1986).
[b] Obtained from data reported by Q. Guo, O. Kato, M. Fujisawa, and A. Yoshida [*Solid State Commun.* **83**, 721 (1992)].

10.6.4 Lowest Indirect Gap

• **Theoretical value**

Table 15.6.12 *Theoretically obtained lowest indirect-gap energy for InN.*

Band gap	Value (eV)	
	a	b
E_g^K ($\Gamma\rightarrow$K)	5.72	6.7
E_g^M ($\Gamma\rightarrow$M)	5.33	5.6
E_g^L ($\Gamma\rightarrow$L)	4.70	5.1
E_g^H ($\Gamma\rightarrow$H)	6.77	
E_g^A ($\Gamma\rightarrow$A)	3.85	3.9

[a] N. E. Christensen and I. Gorczyca, *Phys. Rev. B* **50**, 4397 (1994).
[b] M. van Schilfgaarde, A. Shear, and A.-B. Chen, *J. Cryst. Growth* **178**, 8 (1997).

• **Pressure dependence**

Table 15.6.13 *Theoretically obtained empirical equation for the lowest indirect-gap energy variation with pressure p for InN [6.29].*

$$E_g^{ID}(p) = E_g^{ID}(0) + ap + bp^2$$

E_g^{ID}	Parameter		
	$E_g^{ID}(0)$ (eV)	a (10^{-2} eV/GPa)	b (10^{-4} eV/GPa^2)
E_g^{K} ($\Gamma \rightarrow$K)	5.72	0.19	−0.8
E_g^{M} ($\Gamma \rightarrow$M)	5.33	4.3	−11
E_g^{L} ($\Gamma \rightarrow$L)	4.70	2.3	−7.0
E_g^{H} ($\Gamma \rightarrow$H)	6.77	4.1	−16
E_g^{A} ($\Gamma \rightarrow$A)	3.85	3.3	−8.7

[6.29] N. E. Christensen and I. Gorczyca, *Phys. Rev. B* **50**, 4397 (1994).

15.6.5 Conduction-Valley Energy Separation

• **Theoretical value**

Table 15.6.14 *Theoretically obtained conduction-valley energy separation ΔE_g for InN.*

ΔE_g	Value (eV)	
	a	b
K–Γ	3.68	3.5
M–Γ	3.29	2.3
L–Γ	2.66	1.9
H–Γ	4.73	
A–Γ	1.81	0.9

[a] N. E. Christensen and I. Gorczyca, *Phys. Rev. B* **50**, 4397 (1994).
[b] M. van Schilfgaarde, A. Shear, and A.-B. Chen, *J. Cryst. Growth* **178**, 8 (1997).

15.6.6 Direct–Indirect-Gap Transition Pressure

No detailed data are available for InN.

15.7 ENERGY-BAND STRUCTURE: ELECTRON AND HOLE EFFECTIVE MASSES

15.7.1 Electron Effective Mass: Γ Valley

• Theoretical value

Table 15.7.1 *Theoretical effective masses $m_e^{\perp}$, $m_e^{\parallel}$, and m_e^{Γ} at the Γ valley for InN. $m_e^{\Gamma}=(m_e^{\perp 2}\, m_e^{\parallel})^{1/3}$: density-of-states effective mass.*

$m_e^{\perp}/m_0$	$m_e^{\parallel}/m_0$	m_e^{Γ}/m_0	Ref.
0.124	0.115	0.121	[7.1]
0.10	0.11	0.10	[7.2]
0.10	0.10	0.10	[7.3]
0.10	0.14	0.11	[7.4]
0.1311	0.1190	0.1269	[7.5]

[7.1] T. Yang, S. Nakajima, and S. Sakai, *Jpn. J. Appl. Phys.* **34**, 5912 (1995).
[7.2] Y. C. Yeo, T. C. Chong, and M. F. Li, *J. Appl. Phys.* **83**, 1429 (1998).
[7.3] S. K. Pugh, D. J. Dugdale, S. Brand, and R. A. Abram, *J. Appl. Phys.* **86**, 3768 (1999).
[7.4] S. K. Pugh, D. J. Dugdale, S. Brand, and R. A. Abram, *Semicond. Sci. Technol.* **14**, 23 (1999).
[7.5] M. Goano, E. Bellotti, E. Ghillino, G. Ghione, and K. F. Brennan, *J. Appl. Phys.* **88**, 6467 (2000).

• Experimental value

Table 15.7.2 *Experimental effective mass m_e^{Γ} at the Γ valley for InN. $m_e^{\Gamma}=(m_e^{\perp 2}\, m_e^{\parallel})^{1/3}$: density-of-states effective mass.*

$m_e^{\perp}/m_0$	$m_e^{\parallel}/m_0$	m_e^{Γ}/m_0	Ref.
		0.11	[7.6]
		0.12	[7.7]
0.24			[7.8]
		0.14	[7.9]
		0.07	[7.10]

[7.6] V. A. Tyagi, A. M. Evstigneev, A. N. Krasiko, A. F. Andreeva, and V. Ya. Malakhov, *Sov. Phys. Semicond.* **11**, 1257 (1977).
[7.7] T. Inushima, T. Yaguchi, A. Nagase, A. Iso, and T. Shiraishi, *Inst. Phys. Conf. Ser.* **142**, 971 (1996).
[7.8] T. Inushima, T. Shiraishi, and V. Yu. Davydov, *Solid State Commun.* **110**, 491 (1999).
[7.9] A. Kasic, M. Schubert, Y. Saito, Y. Nanishi, and G. Wagner, *Phys. Rev. B* **65**, 115206 (2002).
[7.10] J. Wu, W. Walukiewicz, W. Shan, K. M. Yu, J. W. Ager III, E. E.Haller, H. Lu, and W. J. Schaff, *Phys. Rev. B* **66**, 201403 (2002).

15.7.2 Electron Effective Mass: Satellite Valley

• Theoretical value

Table 15.7.3 *Theoretical effective masses at the Γ-second minimum (Γ_3^c) and satellite valleys in InN [7.11].*

Valley	Direction	Mass (m_0)
Γ	Γ→M ($m^{\perp}$)	0.2546
	Γ→K (m^{-})	0.2546
	Γ→A ($m^{\parallel}$)	2.0554

Table 15.7.3 *Continued.*

Valley	Direction	Mass (m_0)
K	K→Γ	0.8113
	K→M	0.8040
	K→H	0.4897
M–L	(M–L)→(Γ–A)	1.4449
	(M–L)→(K–H)	0.3571
	(M–L)→M	0.3909
	(M–L)→L	0.3909

[7.11] M. Goano, E. Bellotti, E. Ghillino, G. Ghione, and K. F. Brennan, *J. Appl. Phys.* **88**, 6467 (2000).

15.7.3 Hole Effective Mass

• Luttinger's valence-band parameter

Table 15.7.4 *Theoretical Luttinger's valence-band parameter A_i for InN. A_i (i=1–6) are in units of $\hbar^2/2m_0$ and A_7 is in units of eV/Å. Values in the parentheses correspond to those obtained in the quasi-cubic approximation.*

A_1	A_2	A_3	A_4	A_5	A_6	$\lvert A_7\rvert$	Ref.
–9.28	–0.60	8.68	–4.34	–4.32	–6.08		[7.12]
–9.65	–0.71	8.96	–4.17	–4.18	–5.37	0.33	[7.13]
–8.21	–0.68	7.57	–5.23	–5.11	–5.96		[7.14]
(–10.55)	(–0.45)	(10.11)	(–5.05)	(–4.69)	(–6.11)	(0.00)	
–9.470	–0.641	8.771	–4.332	–4.264	–5.546		[7.15]
–9.15	–0.66	8.50	–4.52	–4.47	–5.74	0.33	Mean value

[7.12] Y. C. Yeo, T. C. Chong, and M. F. Li, *J. Appl. Phys.* **83**, 1429 (1998).
[7.13] S. K. Pugh, D. J. Dugdale, S. Brand, and R. A. Abram, *J. Appl. Phys.* **86**, 3768 (1999).
[7.14] S. K. Pugh, D. J. Dugdale, S. Brand, and R. A. Abram, *Semicond. Sci. Technol.* **14**, 23 (1999).
[7.15] D. J. Dugdale, S. Brand, and R. A. Abram, *Phys. Rev. B* **61**, 12933 (2000).

• Band and density-of-states masses

Table 15.7.5 *Theoretical band and density-of-states hole masses at the A, B, and C valence bands in InN (in m_0). The superscripts $\perp$ and $\parallel$ stand for the perpendicular and parallel to the c-axis, and $m_\alpha^* = (m_\alpha^{\perp 2} m_\alpha^{\parallel})^{1/3}$ denotes the density-of-state mass.*

A			B			C			Ref.
$m_A^\perp$	$m_A^\parallel$	m_A^*	$m_B^\perp$	$m_B^\parallel$	m_B^*	$m_C^\perp$	$m_C^\parallel$	m_C^*	
1.61	1.67	1.63	0.11	1.67	0.27	1.67	0.10	0.65	[7.16]
1.25	1.56	1.35	0.09	1.56	0.23	1.46	0.12	0.63	[7.17]
1.6499	1.4440		0.1721	1.4440		0.3635	0.1067		[7.18]

[7.16] Y. C. Yeo, T. C. Chong, and M. F. Li, *J. Appl. Phys.* **83**, 1429 (1998).
[7.17] S. K. Pugh, D. J. Dugdale, S. Brand, and R. A. Abram, *Semicond. Sci. Technol.* **14**, 23 (1999).
[7.18] M. Goano, E. Bellotti, E. Ghillino, G. Ghione, and K. F. Brennan, *J. Appl. Phys.* **88**, 6467 (2000).

15.8 ELECTRONIC DEFORMATION POTENTIAL

15.8.1 Intravalley Deformation Potential: Γ Point

• Conduction band

Although the intravalley deformation potentials, D_1 and D_2, at the Γ-conduction band have not been reported solely, their combined values with the valence-band deformation potential are available (see below).

• Valence band

Table 15.8.1 *Γ-valence-band deformation potentials C_i's for InN.*

Deformation potential (eV)								Comment
C_1	D_1–C_1	C_2	D_2–C_2	C_3	C_4	C_5	C_6	
	–4.05		–6.67	4.92	–1.79			Calc. [8.1]

[8.1] W. W. Chow, A. F. Wright, A. Girndt, F. Jahnke, and S. W. Koch, *Mat. Res. Soc. Symp. Proc.* **468**, 487 (1997).

• E_0 gap

Table 5.8.2 *Hydrostatic deformation potential a_0^{Γ} for the $E_{0\alpha}$ (α=A, B, or C) gap of InN.*

a_0^{Γ} (eV)	Technique
–4.1	Calc. [8.2]
–2.8	Calc. [8.3]
–9.1	Calc. [8.4]
–2.8	Estimated*

[8.2] N. E. Christensen and I. Gorczyca, *Phys. Rev. B* **50**, 4397 (1994).
[8.3] K. Kim, W. R. L. Lambrecht, and B. Segall, *Phys. Rev. B* **53**, 16310 (1996).
[8.4] S. K. Pugh, D. J. Dugdale, S. Brand, and R. A. Abram, *J. Appl. Phys.* **86**, 3768 (1999).
*From a value of pressure coefficient $dE_{0\alpha}/dp$=2.0×10^{-2} eV/GPa and bulk modulus of B_u=139 GPa.

15.8.2 Intravalley Deformation Potential: High-Symmetry Points

No detailed data are available for InN.

15.8.3 Intervalley Deformation Potential

• Absolute value

Table 15.8.3 *Intervalley deformation potential D_{ij} for electrons in InN.*

D_{ij} (eV/Å)		Ref.
Equivalent intervalley	Nonequivalent intervalley	
10	10	[8.5]
10	10	[8.6]

[8.5] S. K. O'Leary, B. E. Foutz, M. S. Shur, U. V. Bhapkar, and L. F. Eastman, *J. Appl. Phys.* **83**, 826 (1998).
[8.6] B. E. Foutz, S. K. O'Leary, M. S. Shur, and L. F. Eastman, *J. Appl. Phys.* **85**, 7727 (1999).

15.9 ELECTRON AFFINITY AND SCHOTTKY BARRIER HEIGHT

15.9.1 Electron Affinity

No detailed data are available for InN.

15.9.2 Schottky Barrier Height

- **Breakdown voltage**

Table 15.9.1 *Breakdown field E_{BR} in InN [9.1].*

E_{BR} (V/cm)
1.0×10^6

[9.1] See, T. P. Chow, V. Khemka, J. Fedison, N. Ramungul, K. Matocha, Y. Tang, and R. J. Gutmann, *Solid-State Electron.* **44**, 277 (2000).

15.10 OPTICAL PROPERTIES

15.10.1 Summary of Optical Dispersion Relations

- **$\varepsilon(E)$ and $n^*(E)$ spectra**

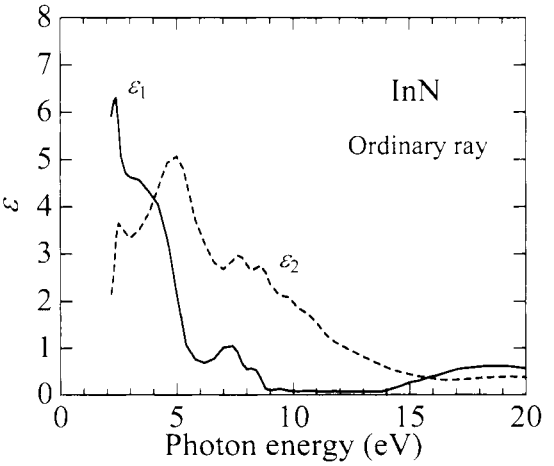

Fig. 15.10.1 Complex dielectric-constant spectra [$\varepsilon(E)=\varepsilon_1(E)+i\varepsilon_2(E)$] for InN at 300 K ($\boldsymbol{E}\perp c$). The numerical data are taken from tabulation by S. Adachi [*Optical Constants of Crystalline and Amorphous Semiconductors: Numerical Data and Graphical Information* (Kluwer Academic, Boston, 1999)].

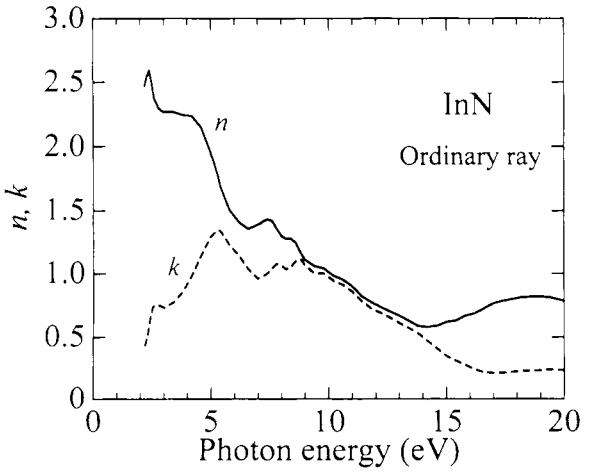

Fig. 15.10.2 Complex refractive-index spectra [$n^*(E)=n(E)+ik(E)$] for InN at 300 K ($\boldsymbol{E}\perp c$). The numerical data are taken from tabulation by S. Adachi [*Optical Constants of Crystalline and Amorphous Semiconductors: Numerical Data and Graphical Information* (Kluwer Academic, Boston, 1999)].

- **$\alpha(E)$ and $R(E)$ spectra**

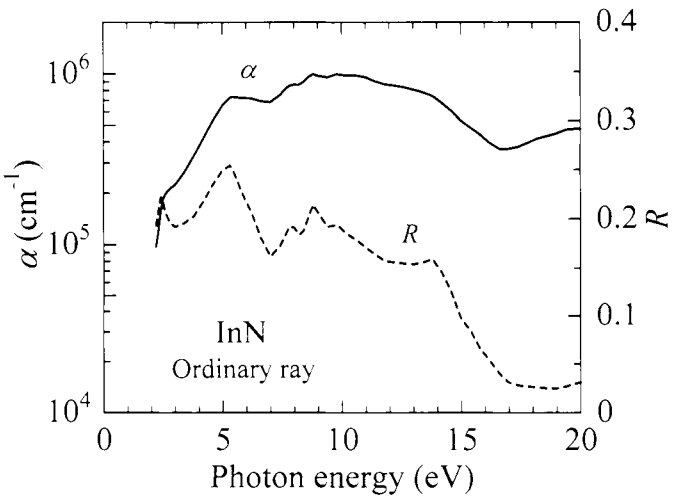

Fig. 15.10.3 (a) Absorption [$\alpha(E)$] and (b) normal-incidence reflectivity spectra [$R(E)$] for InN at 300 K ($\boldsymbol{E}\perp c$). The numerical data are taken from tabulation by S. Adachi [*Optical Constants of Crystalline and Amorphous Semiconductors: Numerical Data and Graphical Information* (Kluwer Academic, Boston, 1999)].

15.10.2 The Reststrahlen Region

Table 15.10.1 *Static and high-frequency dielectric constants ε_s and ε_∞ for InN.*

$\boldsymbol{E}\perp c$		$\boldsymbol{E}\parallel c$		Comment
ε_s	ε_∞	ε_s	ε_∞	
	9.3		9.3	Polycrystal [10.1]
	6.6		6.6	Polycrystal [10.2]
15	8.4	15	8.4	Estimated [10.3]
13.1	8.4	14.4	8.4	Estimated [10.4]
	6.7±0.1		6.7±0.1	Exper. [10.5]

[10.1] V. A. Tyagaĭ, A. M. Evstigneev, A. N. Krasiko, A. F. Andreeva, and V. Ya. Malakhov, *Sov. Phys. Semicond.* **11**, 1257 (1978).
[10.2] K. L. Westra and M. J. Brett, *Thin Solid Films* **192**, 227 (1990).
[10.3] T. L. Tansley, in *Properties of Group III Nitrides*, EMIS Datareviews Series No. 11, edited by J. H. Edgar (INSPEC, London, 1994), p. 35.
[10.4] V. Yu. Davydov, V. V. Emtsev, I. N. Goncharuk, A. N. Smirnov, V. D. Petrikov, V. V. Mamutin, V. A. Vekshin, S. V. Ivanov, M. B. Smirnov, and T. Inushima, *Appl. Phys. Lett.* **75**, 3297 (1999).
[10.5] Isotropically averaged [A. Kasic, M. Schubert, Y. Saito, Y. Nanishi, and G. Wagner, *Phys. Rev. B* **65**, 115206 (2002)].

• **Reststrahlen parameter**

Table 15.10.2 *A set of the reststrahlen parameters for InN at 300 K [10.6].*

$$\varepsilon(\omega) = \varepsilon_\infty \frac{\prod_{i=1}^{2}\left(\omega^2 + i\gamma_{\mathrm{LPP},i}\omega - \omega_{\mathrm{LPP},i}^2\right)}{\left(\omega^2 + i\gamma_{\mathrm{p}}\omega\right)\left(\omega^2 + i\gamma_{\mathrm{TO}}\omega - \omega_{\mathrm{TO}}^2\right)}$$

Parameter	Value	
	$E \perp c$	$E \parallel c$
ε_∞	6.7±0.1	6.7±0.1
ω_{TO} (cm^{-1})	477.1±0.6	443
γ_{TO} (cm^{-1})	4.4±1.0	4.4±1.0
$\gamma_{\mathrm{LPP},1}$ (cm^{-1})	12.1±1.7	12.1±1.7
$\gamma_{\mathrm{LPP},2}$ (cm^{-1})	347±14	347±14
ω_{p} (cm^{-1})	1631±27	1631±27
γ_{p} (cm^{-1})	123±10	123±10

[10.6] A. Kasic, M. Schubert, Y. Saito, Y. Nanishi, and G. Wagner, *Phys. Rev. B* **65**, 115206 (2002).

15.10.3 At or Near the Fundamental Absorption Edge

• **Refractive index**

Table 15.10.3 *Refractive index n near the fundamental absorption edge of InN ($n \sim 3\times10^{20}$ cm^{-3}) at 300 K [10.7].*

E (eV)	λ (μm)	n	E (eV)	λ (μm)	n
0.77	1.60	1.63	1.51	0.82	2.93
0.84	1.48	2.12	1.59	0.78	3.04
1.11	1.12	2.39	1.68	0.74	3.12
1.24	1.00	2.56	1.88	0.66	3.12
1.36	0.91	2.78	2.00	0.62	3.10
1.41	0.88	2.90			

[10.7] V. A. Tyagaĭ, A. M. Evstigneev, A. N. Krasiko, A. F. Andreeva, and V. Ya. Malakhov, *Sov. Phys. Semicond.* **11**, 1257 (1978).

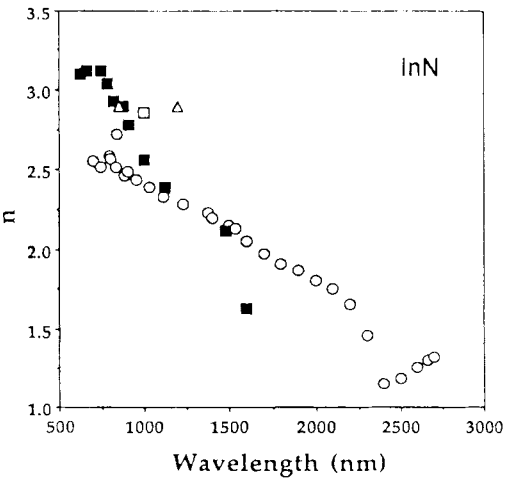

Fig. 15.10.4 Refractive-index dispersion for InN. (○): K. L. Westra and M. J. Brett [*Thin Solid Films* **192**, 227 (1990)], (■): V. A. Tyagaĭ, A. M. Evstigneev, A. N. Krasiko, A. F. Andreeva, and V. Ya. Malakhov [*Sov. Phys. Semicond.* **11**, 1257 (1978)], (□): B. R. Natarajan, A. H. Eltoukhy, J. E. Greene, and T. L. Barr [*Thin Solid Films* **69**, 201 (1980)], (△): H. J. Hovel and J. J. Cuomo [*Appl. Phys. Lett.* **20**, 71 (1972)]. [From K. L. Westra and M. J. Brett, *Thin Solid Films* **192**, 227 (1990).]

• **Refractive index: Pressure dependence**

Table 15.10.4 *Pressure coefficient of the refractive index* $n^{-1}(dn/dp)$ *in the long-wavelength limit for InN.* *

$\frac{1}{n}\frac{dn}{dp}$ (10^{-2} GPa^{-1})	Comment
−0.43	Calc. [10.8]
−3.40	Calc. [10.9]

[10.8] N. E. Christensen and I. Gorczyca, *Phys. Rev. B* **50**, 4397 (1994).
[10.9] B. Abbar, B. Bouhafs, H. Aourag, G. Nouet, and P. Ruterana, *Phys. Status Solidi B* **228**, 457 (2001).
* $n=(2n_{\perp}+n_{\parallel})/3$.

• **Fundamental absorption edge**

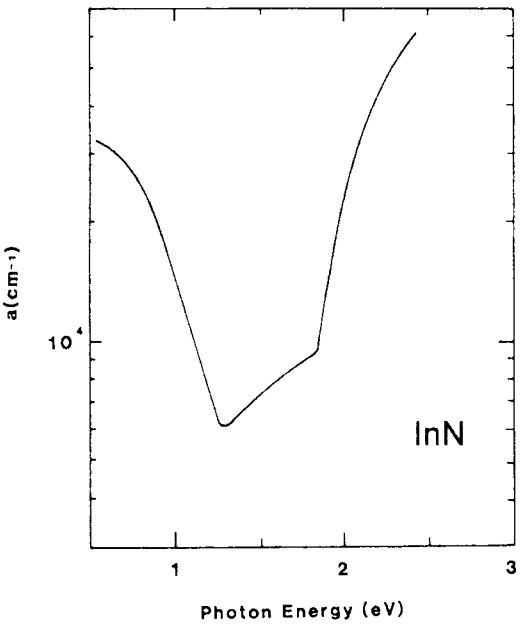

Fig. 15.10.5 Principal features of the optical absorption spectrum for a polycrystalline InN film with $n\sim10^{17}$ cm^{-3}. The range $E>1.8$ eV corresponds to direct interband transitions, $1.2<E<1.8$ eV and $E<1.2$ eV correspond to deep level excitations. [From T. L. Tansley and C. P. Foley, *J. Appl. Phys.* **59**, 3241 (1986).]

15.10.4 The Interband Transition Region

The first-principle calculations of the optical dielectric function of wurtzite and zinc-blende InN have been performed by C. Persson, R. Ahuja, A. F. da Silva, and B. Johansson [*J. Phys.: Condens. Matter* **13**, 8945 (2001)]. Only a few studies have been carried out to obtain the optical spectra in the opaque region of InN [A. Wakahara, T. Tsuchiya, and A. Yoshida, *Vacuum* **41**, 1071 (1990); Q. Guo, O. Kato, M. Fujisawa, and A. Yoshida, *Solid State Commun.* **83**, 721 (1992); Q. Guo, H. Ogawa, and A. Yoshida, *J. Electron Spectrosc. Relat. Phenom.* **79**, 9 (1996); T. Inushima, T. Shiraishi, and V. Yu. Davydov, *Solid State Commun.* **110**, 491 (1999)].

15.10.5 Free-Carrier Absorption and Related Phenomena

No detailed data are available for InN.

15.11 ELASTOOPTIC, ELECTROOPTIC, AND NONLINEAR OPTICAL PROPERTIES

15.11.1 Elastooptic Effect

No detailed data are available for InN.

15.11.2 Linear Electrooptic Constant

No detailed data are available for InN.

15.11.3 Quadratic Electrooptic Constant

No detailed data are available for InN.

15.11.4 Franz–Keldysh Effect

No detailed data are available for InN.

15.11.5 Nonlinear Optical Constant

- **Second-order nonlinear optical susceptibility**

Table 15.11.1 *Second-order nonlinear optical susceptibility d_{ij} in the static limit ($\hbar\omega \rightarrow 0$ eV) for InN.*

d_{ij} (pm/V)			Ref.
d_{15}	d_{31}	d_{33}	
2.8		3.1	[11.1]

[11.1] First-principle full-potential linearized augmented plane-wave method [V. I. Gavrilenko and R. Q. Wu, *Phys. Rev. B* **61**, 2632 (2000)].

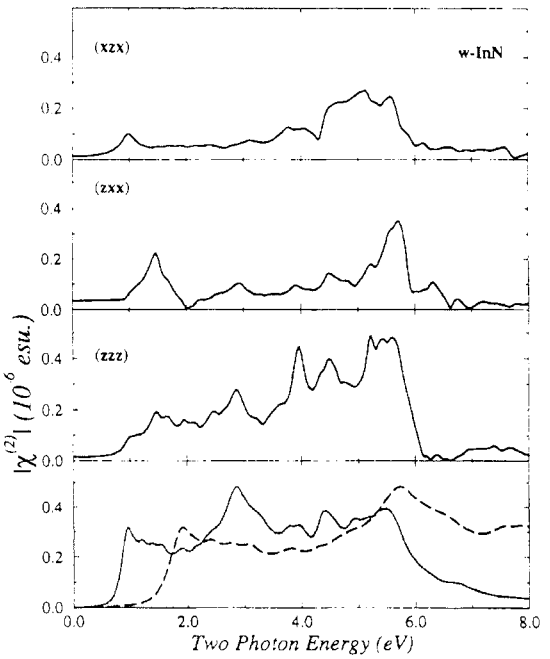

Fig. 15.11.1 Calculated absolute second-order nonlinear optical susceptibility, $|\chi^{(2)}(-2\omega;\omega,\omega)|$, for InN. The calculated $\varepsilon_2(\omega)$ (solid line) and $\varepsilon_2(\omega/2)$ spectra (dashed line) are also shown in the bottom panel. [From V. I. Gavrilenko and R. Q. Wu, *Phys. Rev. B* **61**, 2632 (2000).]

15.12 CARRIER TRANSPORT PROPERTIES

15.12.1 Low-Field Mobility: Electrons

Table 15.12.1 *300-K (μ_{300K}) and peak Hall mobilities (μ_{peak}) for electrons in InN.*

Mobility	Value ($cm^2/V\,s$)	Comment
μ_{300K}	3100	[12.1]
μ_{peak}	5000	T~150 K [12.1]

[12.1] T. L. Tansley and C. P. Foley, *Electron. Lett.* **20**, 1066 (1984).

- **Temperature dependence**

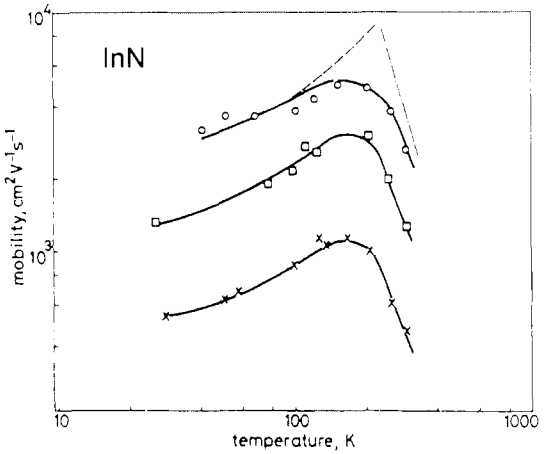

Fig. 15.12.1 Electron mobility against temperature for three InN polycrystalline films deposited by rf sputtering. The dashed and dash-dotted lines represent the theoretical mobilities dominated by ionized-impurity scattering and empirical (polar-optical/space-charge) scattering mechanisms, respectively. [From T. L. Tansley and C. P. Foley, *Electron. Lett.* **20**, 1066 (1984).]

- **Donor concentration (free-carrier) dependence**

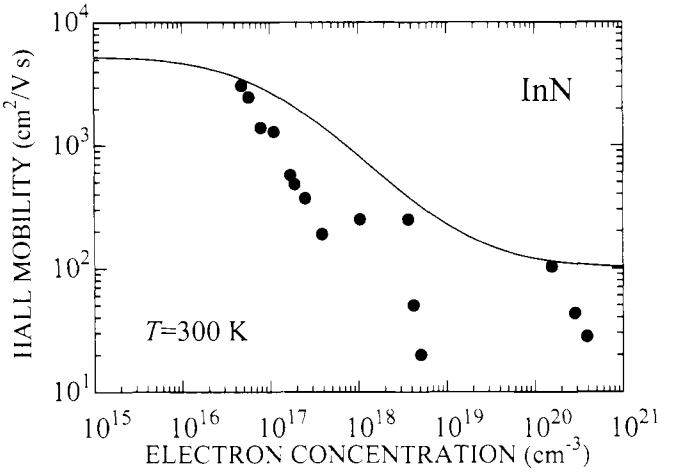

Fig. 15.12.2 Electron Hall mobility μ versus electron concentration n for n-InN at 300 K. The experimental data are taken from various sources. The solid line represents the calculated result with $\mu = 100 + 5300/[1 + (n/10^{17})^{0.80}]$, where n is in cm^{-3} and μ is in $cm^2/V\,s$.

15.12.2 Low-Field Mobility: Holes

No detailed data are available for InN.

15.12.3 High-Field Transport: Electrons

- **Electron scattering rate**

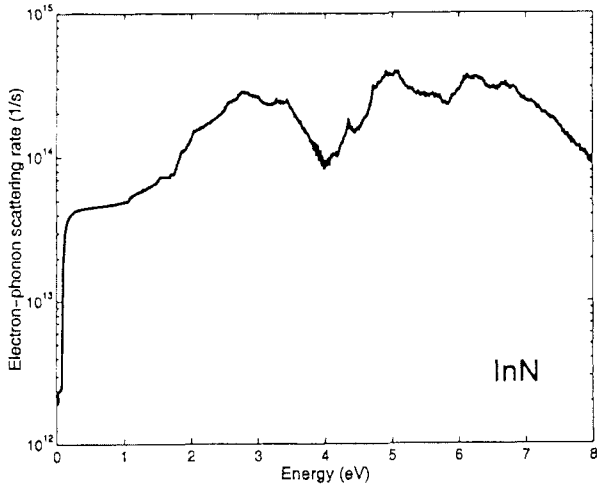

Fig. 15.12.3 Calculated total scattering rate by phonons in InN as a function of electron energy. [From E. Bellotti, B. K. Doshi, K. F. Brennan, J. D. Albrecht, and P. P. Ruden, *J. Appl. Phys.* **85**, 916 (1999).]

- **Electron drift velocity–field characteristic**

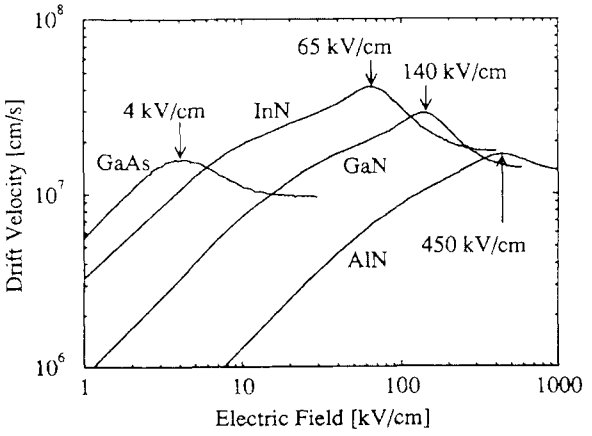

Fig. 15.12.4 Calculated velocity–field characteristic for electrons in InN, together with those in α-GaN, w-AlN, and GaAs (all at 300 K with n=10^{17} cm^{-3}). The arrows indicate the electric fields at which the peak drift velocity is achieved for each velocity–field characteristic. [From B. E. Foutz, S. K. O'Leary, M. S. Shur, and L. F. Eastman, *J. Appl. Phys.* **85**, 7727 (1999).]

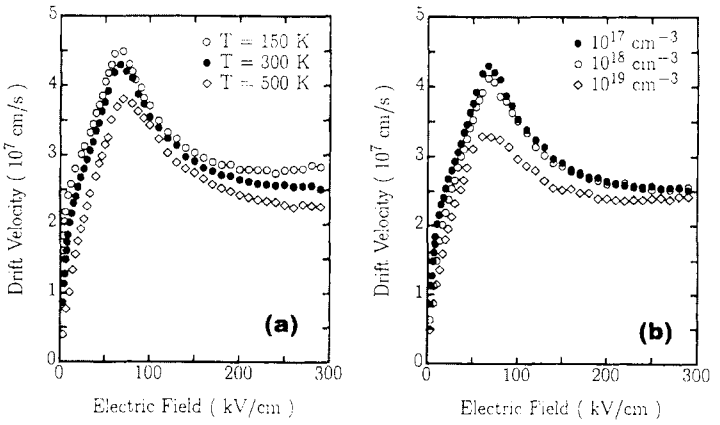

Fig. 15.12.5 Dependence of the electron velocity–field characteristic on (a) temperature (n=1×10^{17} cm^{-3}) and (b) doping concentration for InN (T=300 K). [From S. K. O'Leary, B. E. Foutz, M. S. Shur, U. V. Bhapkar, and L. F. Eastman, *J. Appl. Phys.* **83**, 826 (1998).]

15.12.4 High-Field Transport: Holes

No detailed data are available for InN.

15.12.5 Minority-Carrier Transport: Electrons in *p*-Type Materials

No detailed data are available for InN.

15.12.6 Minority-Carrier Transport: Holes in *n*-Type Materials

No detailed data are available for InN.

15.12.7 Impact Ionization Coefficient

- **Electric-field dependence**

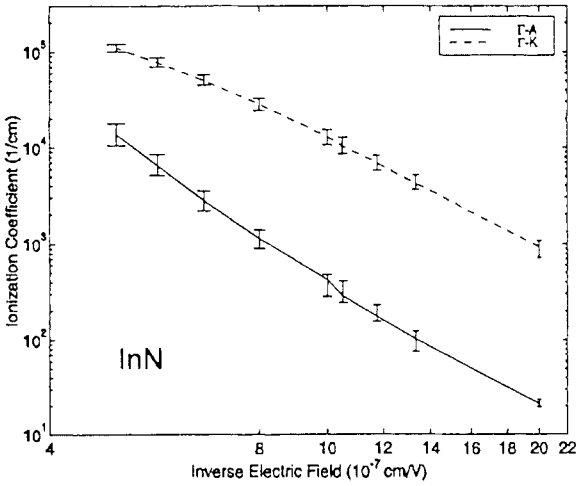

Fig. 15.12.6 Impact ionization coefficient as a function of inverse electric field for electrons in InN as calculated using an ensemble Monte Carlo method. The calculations were performed for an applied electric field along the Γ–A and Γ–K directions. [From E. Bellotti, B. Doshi, K. F. Brennan, and P. P. Ruden, *Mat. Res. Soc. Symp. Proc.* **537**, G6.59 (1999).]